Finite element modeling of bolted connections in thin-walled stainless steel plates under static shear

Tae Soo Kim[a],*, Hitoshi Kuwamura[b]

[a]*Sustainable Building Research Center, Hanyang University, 1271, Sa-1-dong, SangNok-Gu, Ansan, Kyeunggi-do, 425-791, Republic of Korea*
[b]*Department of Architecture, Faculty of Engineering, The University of Tokyo, Tokyo, 113-8656, Japan*

Abstract

The recently performed experimental study indicates that the current Japanese steel design standards (AIJ) cannot be used to predict accurately the ultimate behavior of bolted connections loaded in static shear, which are fabricated from thin-walled (cold-formed) SUS304 austenite stainless steel plates and thus, modified formula for calculating the ultimate strength to account for the mechanical properties of stainless steel and thin-walled steel plates were proposed. In this study, based on the existing test data for calibration and parametric study, finite element (FE) model with three-dimensional solid elements using ABAQUS program is established to investigate the structural behavior of bolted shear connections with thin-walled stainless steel plate. Non-linear material and non-geometric analysis is carried out in order to predict the load–displacement curves of bolted connections. Curling, i.e., out of plane deformation of the ends of connection plates which occurred in test specimens was also observed in FE model without geometric imperfection, the effect of curling on the ultimate strength was examined quantitatively and the failure criteria which is suitable to predict failure modes of bolted connections was proposed. In addition, results of the FE analysis are compared with previous experimental results, failure modes and ultimate strengths predicted by recommended procedures of FE showed a good correlation with those of experimental results and numerical approach was found to provide estimates with reasonable accuracy.
© 2007 Elsevier Ltd. All rights reserved.

Keywords: Thin-walled stainless steel; Bolted connection; Failure mode; Ultimate strength; Curling; Finite element analysis

1. Introduction

Stainless steel has a significant characteristic in its superior corrosion resistance, durability, fire resistance, ease of maintenance, aesthetic appeal, etc., while it has been rarely used in structural members of buildings due to high price. However, in the recent change of social trend from mass production and abundant consumption to ecological coexistence with natural environment, the concept of sustaining a long life of buildings is of much importance in construction engineering. In that context, stainless steel is expected to be promising material for building construction required to durability.

Research for utilizing stainless steel as structural members in building was initiated by Johnson, and Winter

[1] of Cornell University sponsored by AISI in order to conform to the need for design specifications of stainless steels. Based on work results of Johnson and Winter and other many researchers, the first edition of "Specification for the design of light gage cold-formed stainless steel structural members" published by AISI (1968) [2] and "stainless steel cold-formed structural design manual" (1974) [3]. Subsequently, ANSI/ASCE-8-90 specification for design of cold-formed stainless steel structural members (LRFD specification) was also published in 1990 [4]. Recently, Eurocode 3: Part 1.4 (1996) [5], AS/NZS 4673 (2001) [6], and SEI/ASCE 8-02 (2002) [7] standards were published. On the other hand, Japanese research on structural stainless steel for building use dates back only to the late 1980s of virtual growth of economy accompanied with a construction rush of high-rise buildings, which tempted the engineers and researchers to use stainless steel in heavy steel constructions. This led to the

---

*Corresponding author. Tel.: +82 31 400 4690; fax: +82 31 406 7118.
E-mail address: tskim0709@hanyang.ac.kr (T. Soo Kim).

establishment of specification of design and construction of heavy stainless steel structures published by Stainless Steel Building Association of Japan (SSBA) focused on hot-rolled stainless steel [8,9]. In recent years, the most promising use of stainless steel in buildings shows a tendency to be obviously changed in the form of light-weight members relying on its corrosion resistance, which may compensate for the high cost in fabrication as well as material of stainless steel. In fact, thin-walled (cold-formed) stainless steel members are being increasingly used for structural applications [8,10], a design method for thin-walled sections of stainless steel is required in Japan. From this view, Kuwamura et al. [11–15] investigated experimentally local buckling behaviors of stub column and flexural buckling behaviors of centrally loaded columns of thin-walled stainless steel with 1.5 and 3.0 mm thickness designated SUS304 and SUS301L3/4 H with yield strength of 235 and 440 N/mm^2, respectively, and ultimate behaviors of mechanically fastened shear type connections; single shear and double shear connections fabricated from SUS304 flat plates with 1.5 and 3.0 mm thickness. It was recommended that the effective width-thickness ratios should be expressed by different equations for the two strength grades in local buckling, consideration of effective width associated with the reduction of stiffness due to local buckling gave a rational evaluation of the flexural buckling strength of column and based on the fact that current design code (Architectural Institute of Japan; AIJ) tends to overestimate the ultimate strength of thin-walled stainless steel bolted connections, modified formulae for calculating the ultimate strength were proposed, which were found to provide a satisfactory prediction for failure mode and ultimate strength. Based on the research accomplishment with respect to thin-walled stainless steel structures presented above, Stainless Steel Building Association of Japan (SSBA) published "design manual of light-weight stainless steel structures" (2001) [16]. However, when thinner plates (1.5 and 3.0 mm thickness) of single-shear connections or the outside plate of double shear connections with a long end distance (edge distance in the loading direction) curled out of plane, back toward the bolt, the reduction of the load-carrying capacity of bolted connections was observed. It was reported that the curling of ends of plates was not sufficiently considered, and thus, the modified formulae overestimated the ultimate strength of connection with end curling.

Numerical simulation has become more and more popular in almost all research fields, especially, mechanical engineering or civil engineering. Therefore, in order to further investigate the ultimate behaviors such as failure mode and ultimate strength of thin-walled stainless steel bolted connections, in this study, finite element (FE) analysis for the previous test specimens [12] was preformed. Only single plate with free edges in single-shear bolted connections was modeled. Non-linear analysis was carried out in order to extend the range of variables applied in experimental data and investigate the stress/strain component of connection plate in which stress concentration is predicted [17]. Finally, the objective of this paper is to exhibit the test results of representative specimens with distinguished failure mode: net section fracture, end opening fracture and block shear rupture and prove the validation of FEM analysis in predicting the ultimate behaviors of thin-walled stainless steel bolted connections. Parametric studies such as analysis element type, mesh size, loading method, and connection model length were preformed in order to establish the FE analysis model, and FE results showed a good correlation with test results. Furthermore, three failure criteria (FC)which is usually applied in estimating the failure mode of bolted connections were discussed.

2. Reference test results preformed by Kuwamura et al

Experimental research regarding two types of bolted connections: single shear and double shear connections, fabricated from thin-walled stainless steel (austenitic stainless steel type; SUS304) using 1.5 or 3.0 mm thick plate and 12 mm/15 mm diameter bolt (A2-50; SUS common bolt or 10T-SUS; SUS high tensioned bolt) were carried out by Kuwamura et al. (2001) [11,12]. Figs. 1 and 2 display geometry of test specimens and test set-up of specimen (series SA). The both ends of test specimens were gripped through chucks onto a tensile test machine (Amsler typed Universal Testing Machine) by which a tensile force was applied gradually to the test specimen in monotonic displacement control. It should be noted that the experimental data are very important since they can be used for calibration and implementation of numerical analysis. In this FE analysis, Only the thinner plate (1.5 or 3.0 mm thick) out of single-shear connection with both test plates (1.5 or 3.0 mm thick) and rigid plate (6.0 mm thick) was
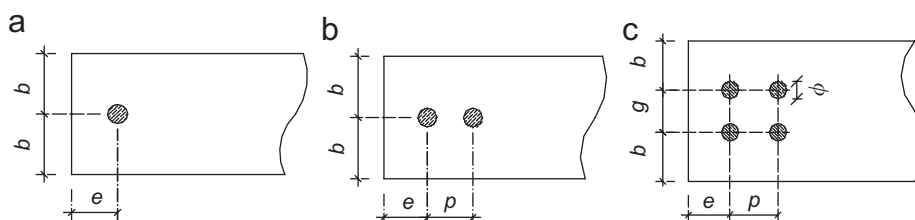
Fig. 1. Geometry of test specimen and notation. (a) Series SA, (b) Series SB, and (c) Series SC.

simulated as depicted in Fig. 1. A total of eight test results which constitute three specimens with 1.5 mm thick plate and five specimens with 3.0 mm thick plate is summarized in Table 1. The object specimens were designed for the following parameters: (1) thickness of plane plate (t): 1.5 and 3.0 mm, (2) 12 mm diameter (d) common bolt and 0.5 mm bolt clearance, (3) 30 mm pitch (p) and gage distance (g), (4) end distance (e) from the center of a bolt hole to the adjacent end of plate in the direction of load; 12, 18, 30 or 60 mm and edge distance (b) perpendicular to the direction of load (fixed values according to all bolt arrangement), (5) three bolt arrangements (Series SA: single bolt; Series SB: two bolts; Series SC: four bolts), as shown in Fig. 1. Three distinct failure modes of connection plate were observed (see Fig. 8): net section fracture (tensile fracture, henceforth, is named by N), end opening fracture (end tear-out fracture or shear-out fracture, E) and block shear rupture (a combined tensile fracture and edge shearing, B) and failure mode of each specimen obtained from the test results can be clearly discerned, except specimen SC2-1 which has combined failure mode; i.e., end tear-out (E) occurs first at the bolt hole in the first column of bolt nearest the end of specimen and tensile fracture subsequently occurs in the net section between bolt holes (the second column of bolt), finally led to block shear rupture mode (B) where ultimate strength of specimen SC2-1 was reached. Moreover, test specimens such as SB1-4, SC1-4, SC2-3 and SC2-4 with a relatively long end distance curled out of plane, as shown in Fig. 8(e).

Fig. 2. Test set up for specimen (Series SA)

3. FE modeling

3.1. General

FE analysis provides a relatively inexpensive and time efficient alternative compared with physical experiments. It is essential to have a sound test data on which to calibrate a FE model [18]. If the validity of FE analysis is assured, it is possible to investigate the structural behavior against a wide range of parameters with the FE model.

In this research, the ABAQUS (Version 6.4) FE package installed on steel structure laboratory in the Department of Architecture, The University of Tokyo, was utilized to predict the structural behaviors (load–displacement curves) of bolted connections fabricated from thin-walled stainless steel under shear loading. ABAQUS is an excellent program that can incorporate material, geometric and boundary non-linearitiy caused by non-linear elasticity, plasticity (strain hardening), large displacement, contact problem, etc [18–21]. The behavior of bolted connection in thin stainless steel plate was estimated to be highly non-linear from test results [11,12]. In the following sections, the procedures for implementation of a FE model with acceptable accuracy using ABAQUS program were described. The non-linear geometry parameter (*NLGEOM = ON) was set to deal with the large displacement analysis in ABAQUS step module [19].

3.2. Material modeling

The nominal stress–nominal strain (σ_n–ε_n) curve obtained from conventional coupon tests does not give a true indication of the deformation characteristics of a material at higher strain as it is based entirely on the original dimensions of the specimens, while in reality, the dimensions of the material change continuously during coupon test. Therefore, it is required that the definitions of nominal stress, F/A_0, and nominal strain, $\Delta l/l_0$, where subscript 0 indicates a value from the undeformed state of the material, be replaced by new measures (true stress and true strain) of stress and strain that account for the change of dimension. The material properties were input into the ABAQUS model as a set of points on the stress–strain

Table 1
Test specimens and test result

Series	Specimen	Thicknesst (mm)		End distance	Edge distance	Width	Failure mode	P_{ue} (kN)
		Nominal	Actural	e (mm)	B (mm)	w (mm)		
SA	SA1-1	1.5	1.46	12	25	50	E	12.28
SB	SB1-4		1.46	60	25	50	N	43.34
SC	SC1-4		1.45	60	55	140	B	79.53
SA	SA2-2	3.0	2.94	18	25	50	E	48.05
SB	SB2-4		2.90	60	25	50	N	85.62
	SC2-1		2.89	12	55	140	E→B	115.62
SC	SC2-3		2.91	30	55	140	B	162.34
	SC2-4		2.90	60	55	140	B	163.3

curve. ABAQUS uses true stress and true strain (σ_t–ε_t), and hence the values of nominal stress and nominal strain are converted to true stress and true strain as the plastic material data using the following Equations [19,21–23]:

$$\sigma_t = \sigma_n(1 + \varepsilon_t) \tag{1}$$

$$\varepsilon_t = \ln(1 + \varepsilon_t) \tag{2}$$

Figs. 3(a) and (b) show the stress–strain curves of SUS304 material with 1.5 and 3.0 mm thick, respectively. Table 2 summarizes the measured material properties of SUS304 steel [11].

The material behavior provided by ABAQUS allows a multilinear stress–strain curve to be used. The first part of the multilinear curve represents the elastic part up to the proportional limit stress (yield strength) measured Young's modulus (E) and Poisson's ratio ($v = 0.3$). Yield strength of stainless steel for design is defined as 0.1% proof stress for coupon test in Stainless Steel Building Association of Japan [8,9]. Since FE analysis is expected to involve large inelastic strain, the plastic true strain should be input in material property instead of total true strain (ε_t), which decomposes into elastic and plastic components. The plastic strain (ε_{pl}) is obtained by subtracting the elastic strain (ε_{et}) from the value of total strain (ε_t) as defined by [19,20]:

$$\varepsilon_{pl} = \varepsilon_t - \varepsilon_{et} = \varepsilon_t - \frac{\sigma_t}{E}, \tag{3}$$

where, ε_{pl} is the true plastic strain (logarithmic plastic strain), ε_t the total true strain and ε_{et} the true elastic strain.

Due to large local deformation of the thin-walled steel plate around the bolt hole in direct contact with bolt shanks, plasticity of thin SUS304 material is considered by

incorporating the von Mises yield criterion and the Prandtl–Reuss flow rule with isotropic hardening rule [17,18,24]. To put them more concretely, Mises yield criterion determines the stress level at the beginning of yielding and the associated plastic flow relates the stress increment to strain increments during plastic deformation. Isotropic hardening rule allows the yield surface to change size uniformly in all directions such that the yield stress increases (or decreases) in all stress directions as plastic straining occurs [17,18].

3.3. Geometry and simplification of model

The objective of FEM analysis is not to describe reality as accurately as possible, but to find the simplest model resulting in a sufficiently accurate description of reality, Thus, only thinner plate (1.5 or 3.0 mm thick) in single-shear connections with both 1.5 or 3.0 mm thick plate, which can be deformable under loading and 6.0 mm thick plate (rigid plate to set up), which never deform is modeled in order to curtail the run time by minimizing the total number of nodes and elements as displayed in Fig. 1. Though the whole length of all specimens was cut out at 300 mm, the effective length that subtracts grip part length from the whole length was not identical for all specimens due to different grip sizes. Furthermore, the influence of specimen length on the failure mode and ultimate strength of bolted connection was analyzed in Section 4.3, where the desirable model length for FE analysis was recommended. Based on the symmetry considerations of Series SC specimen with even-numbered bolt arrangement in the perpendicular to the direction of load, only half width of the specimen was modeled and symmetric conditions
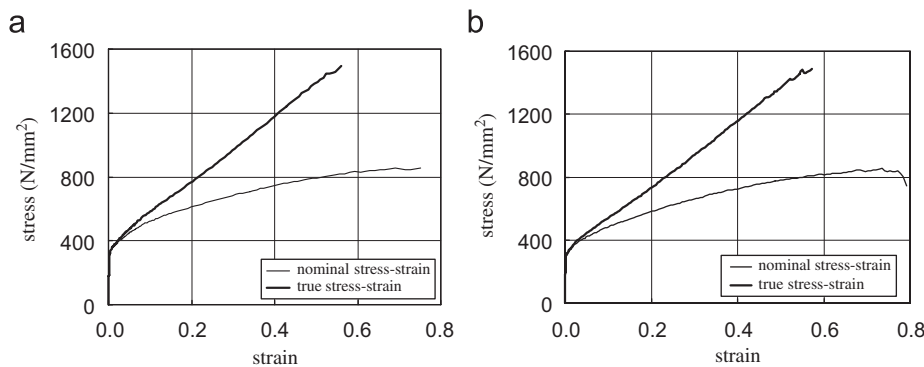
Fig. 3. Stress–strain curves of SUS304. (a) 1.5 mm thickness plate and (b) 3.0 mm thickness plate.

Table 2
Measured material properties of thin-walled SUS304 steel in coupon tests

Steel grade	Actural thickness t(mm)	Elastic modulus E (kN/mm^2)	0.1%offset stress σ_y (N/mm^2)	Tensile stress σ_u (N/mm^2)	Yield ratio σ_y/σ_u YR (%)	Elongation limit (EL) (%)
SUS304	1.45	198	313	862.09	36.3	62.0
	2.92	204	288	842.35	34.2	63.0

(symmetric plane is 1–3 plane) was applied to all nodes of the middle section of plane as shown in Fig. 5(b) [18].

As the shear section of M12 ordinary bolt, which contacts directly with the bolt hole of plane plate was designed to be located at the non-threaded part of bolt shank [12], the bolt was assumed to be threadless in FE modeling. The common bolts used in test specimens of bolted shear connection were snug-tightened, thus, the plate resists the applied force directly near the area of the hole. Since the specimen was bearing type connection, bolt pre-tension was not simulated. In addition, no friction between plate and washer and between specimen plate and rigid plate was assumed [12,25,26]. The 3-axis direction (thickness direction) displacement in the vicinity of bolt hole was set to be fixed ($u_3 = 0$) by constraining the associated node to account for the restraining effect of the bolt head, nut and washer (see Fig. 5) [26].

3.4. FE type and meshing

ABAQUS has several element types suitable for FE analysis such as solid element, shell element, beam element, membrane element, truss element, etc. [19]. However, the main purpose of analysis is to predict failure mode and ultimate strength of thin-walled bolted connections which accompany inelastic local instabilities and curling of plate. Beam, membrane and truss elements may not be proper for this type of connection model. In this paper, two types of elements for connection plate: i.e., shell element (S4R) and solid element (C3D8R) were employed. The S4R is defined as a four-node doubly curved general-purpose, finite membrane strain, first-order (linear) reduced integration shell element with hourglass control. The general-purpose shell allows transverse shear deformation and is valid for thick and thin shell problems. It uses thick shell theory as the shell thickness increases and becomes discrete Kirchhoff thin shell element as the thickness decreases; the transverse shear deformation becomes very small as the shell thickness decreases. In addition, reduced integration (1 G point) with hourglass usually provides more accurate results and significantly reduces running time, especially in three-dimensioned model. S4R element has six degree-of-freedoms per node: u_1, u_2, u_3, ϕ_1, ϕ_2, ϕ_3, and as the element output, the stress components are as follows: S11 (σ_{11}; local 11 direct stress), S22 (σ_{22}; local 22 direct stress), S12 (τ_{11}; local 12 shear stress).

The C3D8R is defined as a three-dimensional, hexahedral eight-node linear brick, reduced integration with hourglass control solid element and first-order (linear) interpolation element. The solid elements in ABAQUS can be used for linear analysis and for complex nonlinear analyses involving contact, plasticity, and large deformations. First-order element is recommended when large strains or very high strain gradient are expected. Reduced integration uses a lower-order integration to form the element stiffness, but the mass matrix and distributed loadings are still integrated exactly. Reduced integration

reduces running time, especially in three dimensions. For example, element type C3D8 has eight integration points, while C3D8R has only 1 G point. In addition, linear reduced-integration element C3D8R is very tolerant of distortion; therefore, use a fine mesh of these elements in any simulation where distortion levels may be high. Hourglassing can be a problem with first-order, reduced-integration element, namely, C3D8R in stress or displacement analysis. Since the elements have only one integration point, it is possible for them to distort in such a way that the strains calculated at the integration point are all zero, which, in turn, leads to uncontrolled distortion of the mesh. This deformation mode is zero-energy mode, because no strain energy is generated by element distortion. The zero energy mode can propagate through the mesh, producing inaccurate results. Therefore, first-order, reduced-integration elements in ABAQUS include hourglass control that an additional artificial stiffness is added to the element in order to prevent excessive deformation [19,23]. C3D8R element has three translational degree-of-freedoms per node: u_1, u_2, u_3, and as the element output, the stress components are as follows: S11 (σ_{11}; local 11 direct stress), S22 (σ_{22}; local 22 direct stress), S33 (σ_{33}; local 33 direct stress), S12 (τ_{12}; local 12 shear stress), S23 (τ_{23}; local 23 shear stress), S13 (τ_{13}; local 13 shear stress).

In experimental results of Kuwamura et al., since measured ultimate strength of bolt shear failure showed a good agreement with that of current design standard, it is assumed that failure does not take place in the bolt itself: namely, this FE analysis does not aim at modeling the bolt failure. Accordingly, the bolt shank is idealized as rigid cylindrical body (revolved analytical rigid surface) [21,22,27] or a linear elastic material with the same Young's modulus as that of the connected SUS304 steel plate [17,18].

Figs. 4(a) and (b) show finite element mesh of the whole plate model for shell element and solid element, respectively. Mesh area is divided into two; one part around the
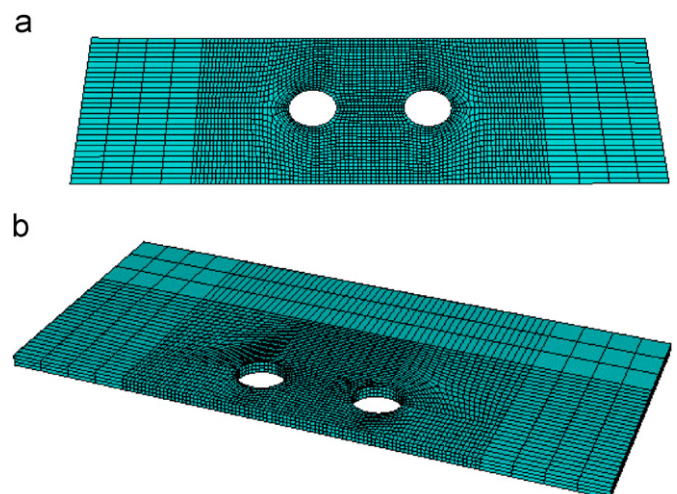
Fig. 4. Finite element mesh (a fine mesh near the bolt hole). (a) Shell element mesh (SB2-4) and (b) Solid element mesh (SC2-4).

bolt holes (30 mm area from the center of bolt hole) and the other part (the remaining part) except the vicinity of the bolt holes, as illustrated in Fig. 4, with each different mesh density. The mesh is refined locally in the vicinity of the bolt hole for improved resolution of stress and strain due to the presence of the stress concentration [17], based on the thickness of plate (t). It is difficult to FEs to get reasonable stress and strain around the holes. Thus, consideration about the accuracy of final results and the total running time should be carefully taken according to the difference of mesh size in each element type (S4R and C3D8R), especially for non-linear FE analysis. In this study, mesh size of the stress concentration part varied through the plate surface: $t/2$, $t/3$, $t/6$ for shell element, through surface by thickness $t/2 \times t/1$, $t/2 \times t/2$, $t/3 \times t/3$, $t/3 \times t/4$, etc. for solid element as shown in Tables 2 and 3.

3.5. Boundary and load conditions

In case that loading is applied to the bolt as displayed in Fig. 5(b), nodes along the right edge of FE plate model are fixed in the 1,2,3 direction. For shell element, all degree-of-freedoms are zero: u_1, u_2, u_3, ϕ_1, ϕ_2, ϕ_3, $= 0$ and for solid element, u_1, u_2, $u_3 = 0$. Nodes along symmetry plane (1–3 axis plane) shown in Fig. 5 are fixed with symmetric geometric boundary conditions (u_2, ϕ_1, $\phi_3 = 0$). Rigid body reference point (marked $+$) is assigned to the bottom edge of bolt shank so that motion or constraints applied to the rigid body reference point can be applied to the entire rigid surface, namely bolt element. Reference point is fixed in displacement and rotation of all directions except direction of load (u_1,) in order to prevent rotation and bolt tilting. As already mentioned above, the circumference of bolt hole is fixed in the displacement of thickness direction (u_3, $= 0$) owing to restraining effect of the bolt head, nut and washer [26,28].

Bolt shank and bolt hole are simulated as bearing contact in FE model. Contact between the bolt shank and bolt hole is defined using the CONTACT PAIRS option (surface-based contact) in ABAQUS. Load is fully transferred to the plate by bearing the bolt against the

bolt hole. Therefore, no friction between the bolt surface and bolt hole is assumed [26].

Two loading patterns such as the force control and the displacement control are commonly used in FE analysis as well as experimental research. In this paper, loading to FE model is applied with the displacement control that enforces prescribed displacement at reference point to reflect on the sudden strength reduction during analysis. It can be seen that existing tests by Kuwamura et al. adopted the loading pattern of enforced displacement control [11,12]. Two types of loading method are tried so as to investigate the influence on the ultimate behavior according to the difference of loading position. One type is assigned to the reference point located at the exterior place apart from right edge of plate mode shown in Fig. 5(a) and for the other, to the reference point on the bolt shank shown in Fig. 5(b). Using the *RIGID BODY option (rigid body constraint), the motion of right edge of plate (slave surface) is constrained to the motion of the reference point (master point) as depicted in Fig. 5(a) and relative position of the nodes in plate end that are tied to the reference point can be remain constant throughout the analysis.

3.6. FC and curling

3.6.1. Failure criteria

The ultimate strength of bolted connections is eventually governed by cracking of the connection plate material. Most of the failures in test specimens were seen to initiate at the edge of the plate section closest to leading bolt hole and finally led to the ultimate state. It is necessary to present the appropriate criteria to predict the failure mode of bolted connection such as net section failure, end opening fracture and block shear rupture in the FE analysis. There are various failure criteria (FC) employed in the procedures of FE analysis [17,27–29], which actually define fracture of bolted connections based on stress or strain; e.g., direct or shear stress (FC1), equivalent stress (FC2) and equivalent plastic strain (FC3). In order to investigate the stress and strain of the part at which the crack initiates and stress is concentrated, reference node is assigned at the plate model as shown in Fig. 6 When the

Table 3
FE results of shell element S4R according to mesh size

Speimen	FE analysis				Experiment			P_{ua}/P_{ue}
	Mesh size W (mm)	P_{ua} (kN)	Failure mode (FC1)	Remarks	P_{ue} (kN)	Failure mode	Remarks	
SA2-2	$t/6$	49.32	E	—	48.05	E	—	1.03
	$t/3$	55.11	E					1.15
	$t/2$	69.70	E					1.45
SB2-4	$t/6$	84.46	N	—	85.62	N	—	0.99
	$t/3$	84.94	N					0.99
	$t/2$	85.80	N					1.00
SC2-4	$t/6$	199.55	B	—	162.32	B	Curled	1.23
	$t/3$	202.82	B					1.25
	$t/2$	204.50	B					1.26
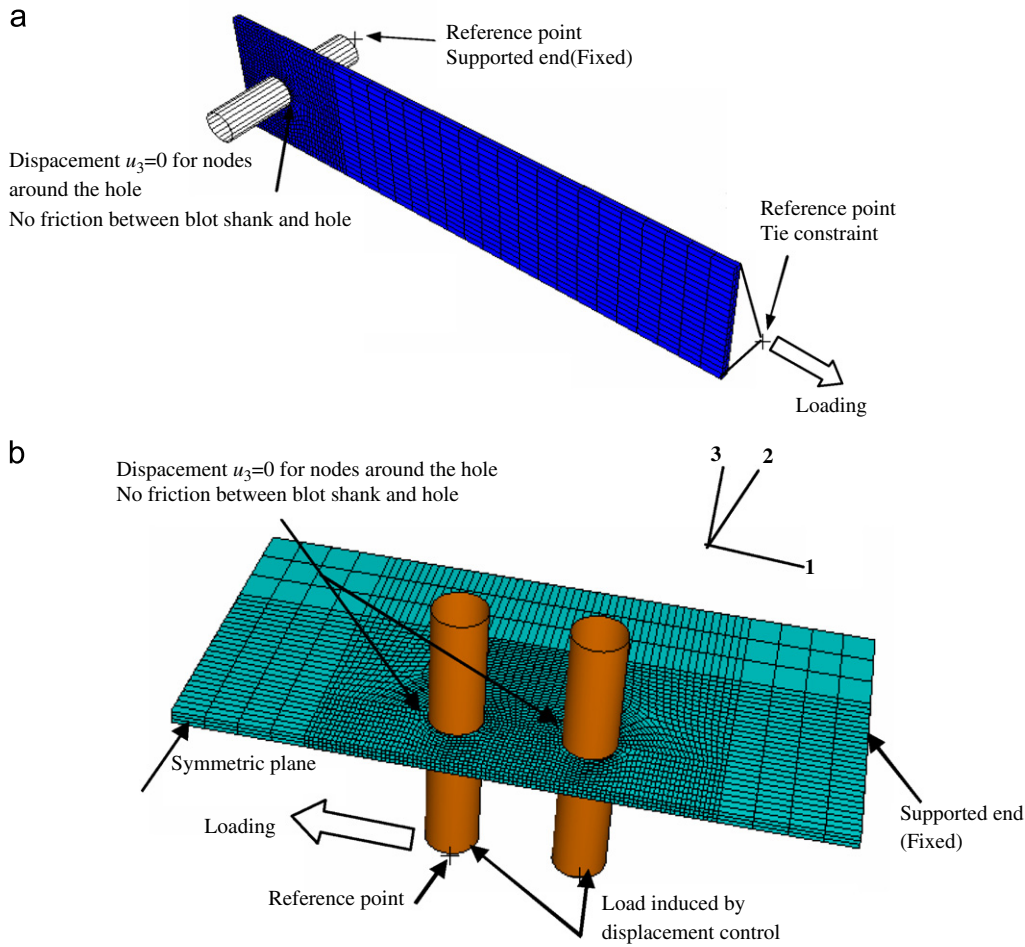
Fig. 5. Details of finite element model (Solid element). (a) SA2-2 and (b) SC2-4.
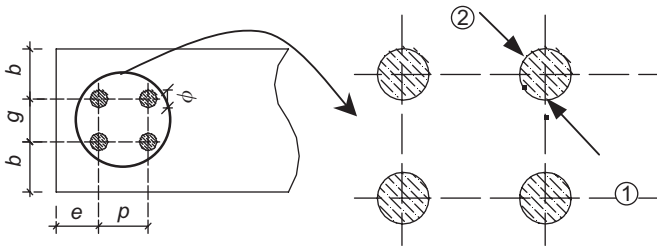
Fig. 6. Location of stress and strain investigation.

stress or strain obtained in this node reaches the threshold value ($\sigma_{t\,max}$ or $\varepsilon_{t\,max}$), which corresponds to the maximum true stress ($\sigma_{t\,max}$) or maximum true strain ($\varepsilon_{t\,max}$) converted from tensile strength ($\sigma_{n\,max}$) or uniform elongation ($\varepsilon_{n\,max}$), It is assumed that crack of the section near the bolt hole starts to occur and then propagates through the model. Net section failure is critical in connection plate with narrow plate width and the failure zone is developed across the centerline of the bolt hole in the net section of plate. End opening fracture (shear-out failure) is observed only when the end distance in the direction of load is short and is characterized by large shear stress between the side of bolt hole and end edge of plate.

Block shear rupture is typically defined as combination of the fracture/yielding of section perpendicular to the direction of load and the shear fracture of section parallel to the direction of load [12,31,32]. The ultimate strength (failure load) in the analysis is assumed to be the maximum load obtained from load-displacement curve [30].

The FC described above can be simplified as follows:

FC 1 (direct stress or shear stress):

$$\frac{\sigma_{ii}}{\sigma_{t\,max}} \geqslant 1.0 \text{ and } \frac{\tau_{ij}}{\tau_{t\,max}} \geqslant 1.0. \tag{4}$$

FC 2 (equivalent stress):

$$\frac{\sigma_{eq}}{\sigma_{t\,max}} \geqslant 1.0. \tag{5}$$

FC 3 (equivalent plastic strain):

$$\frac{\varepsilon_{eq}^{p}}{\varepsilon_{t\,max}} \geqslant 1.0. \tag{6}$$

where σ_{ii} is the direct stress, τ_{ij} the shear stress, $\sigma_{t\,max}$ the maximum true stress (ultimate stress), $\tau_{t\,max}(= \sigma_{t\,max}/\sqrt{3})$ the maximum true shear stress, σ_{eq} the equivalent von Mises stress, ε_{eq}^{p} the total equivalent plastic strain, $\varepsilon_{t\,max}$ the maximum true strain (ultimate strain).

If von Mises yield criterion is adopted, σ_{eq} and ε_{eq}^p can be expressed by the following equations, respectively.

In case of the equivalent stress (σ_{eq}):

For the initial yield condition $\sigma \leqslant \sigma_y$ (elastic area), equivalent elastic stress is given as

$$\sigma_{eq}^e = \sqrt{\frac{3}{2}\sigma'_{ij}\sigma'_{ij}} \tag{7}$$

$$= \frac{1}{\sqrt{2}}\sqrt{(\sigma_{11}-\sigma_{22})^2+(\sigma_{22}-\sigma_{33})^2+(\sigma_{33}-\sigma_{11})^2+6(\tau_{12}^2+\tau_{23}^2+\tau_{31}^2)}, \tag{8}$$

where, σ'_{ij} is the deviatoric stress, $= \sigma_{ij} - \frac{1}{3}\sigma_{ii}\delta_{ij}$, σ_{ii} the hydrostatic stress (mean stress),

δ_{ij} the Kronecker delta ($\delta_{ij} = 1$ for $i = j$, and $\delta_{ij} = 0$ for $i \neq j$).

For the subsequent yield condition $\sigma \geqslant \sigma_y$ (plastic area), equivalent plastic stress is given as

$$\sigma_{eq}^p = \sqrt{\frac{3}{2}\sigma'_{ij}\sigma'_{ij} - \sigma_y^2\varepsilon_{eq}^p}, \tag{9}$$

where, σ_y is the yield stress, ε_{eq}^p the equivalent plastic strain.

In case of the equivalent plastic strain (ε_{eq}^p),

$$\varepsilon_{eq}^p = \int d\varepsilon_{eq}^p, \tag{10}$$

$$d\varepsilon_{eq}^p = \sqrt{\frac{2}{3}d\varepsilon_{ij}^p d\varepsilon_{ij}^p} \tag{11}$$

$$= \frac{\sqrt{2}}{3}\sqrt{(d\varepsilon_{11}-d\varepsilon_{22})^2+(d\varepsilon_{22}-d\varepsilon_{33})^2+(d\varepsilon_{33}-d\varepsilon_{11})^2+\frac{3}{2}(d\gamma_{12}^2+d\gamma_{23}^2+d\gamma_{31}^2)}. \tag{12}$$

3.6.2. Curling

As long as out of plane deformation in the free end is not restrained, when the end distance (e) or edge distance (b) in the thin-walled steel connections becomes longer, curling of the ends of plate may occur as observed in specimen SC2-4 of Fig. 8(e). It is reported that many of the single-shear specimens tested by Winter (flat lapped joints, 1956) [33] and Chong et al. (lapped joints with lips, 1975) [34] showed considerable curling and bending out of the original plane but they report that the load carrying capacity of light-gage steel connections was little affected by such a curling. As observed from test results and FE modeling of bolted connections for cold-formed steel strips by Chung et al. [17], strip curling occurred before the peak load was reached. While, strip curling was unlikely to take place in typical connection arrangements in practice, and accurate modeling of strip curling was considered not to be critical. In addition, in the experimental research performed by Kuwamura et al. (2001) [11,12], curling of the ends of plate also occurred. Modified formula for the ultimate strength of fastener connections without curling of thin stainless steel plates proposed were found to provide a satisfactory prediction for failure mode and ultimate strength, but

strength reduction caused by curling was not sufficiently taken into account, then the modified formula resulted in overestimating the ultimate strength for specimens with end curling. Thus, in this study, the FE analysis of bolted connection for the thin-walled stainless steel plate was performed in order to present the curling model and investigate influence of the curling on the ultimate strength of bolted connections.

4. FE analysis results and parametric study

A total of eight bolted connections fabricated from thin-walled stainless steel; SUS304 (1.5 mm thick and 3.0 mm thick plate) was modeled to predict the failure mode and ultimate strength of bolted connections using FE analysis. At first, in order to verify the validity of the FE model, comparisons between the test results and analysis results obtained from various parametric studies with only five target specimens of 3.0 thickness plate (SA2-2, SB2-4, SC2-1, SC2-3 and SC2-4) are made in the following.

4.1. Influence of element type and mesh size

Tables 3–5 show a comparison between the test results and FE analysis results obtained from connection model with two types of elements (shell element: S4R and solid element: C3D8R) and mesh size discussed in Section 3.4. Based on the results derived from the following section,

whole length of model is 150 mm, enforced displacement (loading) is assigned at the reference point of bolt shank and failure criterion 1 (FC1, refer to Eq. (4)) is applied to predict the failure mode of bolted connections.

When element type S4R is applied to the plate model, the failure modes of FE results show a good agreement with those of the test results regardless of mesh size. However, curling observed in test specimen SC2-4 did not occur in FE analysis as can be seen in Table 3. Since in-plane stress resists against external force in shell element, it is apparent that out of curling will not occur for bolted connections modeled by shell element without eccentric loading. To the contrary, SC2-4 designated by solid element shows considerable curling and failure mode predicted from FE results are in a good agreement with those of test results as shown in Table 4. The discrepancy between the FE result and test result for SC2-3 with respect to curling is discussed in following the section (refer to Section 4.4). In brief, it is found that curling observed at the end of plate for SC2-3 specimen tested, but from the FE results, since the curling is proved to occur after the ultimate load is reached, the curling observed in SC2-3 can have negligible influence on the ultimate strength.

Table 4
FE results of solid element C3D8R according to mesh size

Speimen	FE analysis				Experiment			P_{ua}/P_{ue}
	Mesh size T × W (mm)	P_{ua} (kN)	Failure mode (FC1)	Remarks	P_{ue} (kN)	Failure mode	Remarks	
SA2-2	$t/3 \times t/3$	44.94	E					0.94
	$t/2 \times t/2$	44.25	E	–	48.05	E	–	0.92
	$t/2 \times t/1$	44.41	E					0.92
SB2-4	$t/4 \times t/6$	85.74	N		86.62	N	–	1.00
	$t/3 \times t/4$	86.32	N					1.00
	$t/3 \times t/3$	86.94	N	–				1.00
	$t/2 \times t/2$	88.38	N					1.02
	$t/2 \times t/1$	87.89	N					1.01
SC2-1	$t/4 \times t/6$	128.70	E→B		98.05→115.62	E→B	–	1.11
	$t/3 \times t/4$	129.42	E→B					1.12
	$t/3 \times t/3$	130.92	E→B	–				1.13
	$t/2 \times t/2$	132.16	E→B					1.14
	$t/2 \times t/1$	143.64	N					1.24
SC2-3	$t/3 \times t/4$	175.55	B					1.09
	$t/3 \times t/3$	176.69	B	Curled	161.59	B	Curled	1.09
	$t/2 \times t/2$	173.92	E→B					1.08
	$t/2 \times t/1$	174.77	B					1.08
SC2-4	$t/3 \times t/4$	201.90	B	–				1.24
	$t/3 \times t/3$	152.79	B	Curled				0.94
	$t/2 \times t/2$	204.84	B	–	162.32	B	Curled	1.26
	$t/2 \times t/1$	187.31	B	–				1.15

Table 5
Detailed analysis of SC2-4 (solid element) according to mesh size

Speimen	FE analysis				Experiment			P_{ua}/P_{ue}
	Mesh size T × W (mm)	P_{ua} (kN)	Failure mode (FC1)	Remarks	P_{ue} (kN)	Failure mode	Remarks	
SC2-4	$t/6 \times t/3$	152.79	B	Curled				0.94
	$t/3 \times t/3$	155.68	B	Curled	162.32	B	Curled	0.96
	$t/3 \times t/2$	150.60	B	Curled				0.93
	$t/2 \times t/3$	154.93	B	Curled				0.95

For the whole plane plate of bolted connections, different mesh densities were adopted according to stress concentration and element type (see Section 3.4). Shell element (SA2-2 and SB2-4) which are not accompanied by curling are required to have mesh size less than $t/3$ mm through the plate surface so that FE analysis can predict appropriately the ultimate behavior of bolted connection as presented in Table 3. For the solid element type (C3D8R), it is found that the specimens SA2-2, SB2-4 and SC2-1 with no curling need the mesh size less than $t/2 \times t/2$ mm (surface by thickness) against the vicinity of bolt hole and the specimens SC2-3 and SC2-4 with curling are recommended to be divided by mesh size $t/3 \times t/3$ mm (surface by thickness) as given in Table 4. In the FE result for specimen SC2-4, As can be seen in Table 4, curling occurred at only $t/3 \times t/3$ mm mesh size. Therefore, additional investigation about mesh size effect was conducted to confirm the accuracy of the prediction of curling by FE analysis. The FE results are summarized in Table 5. It is interesting to note that the mesh refinement study (mesh size) is very vital to predict the accurate

behavior of thin-walled bolted connections and estimate the influence of curling on the ultimate strength. In this paper, the element type C3D8R is finally adopted, which is much more suitable to embody the ultimate behavior of bolted connection for thin-walled stainless steel.

4.2. Influence of loading position

The influence of loading position on the overall behavior is analyzed in this section. Section 3.4 presents two kinds of loading patterns: one is assigned to the reference point on the bolt shank and the other is assigned to the reference point located at the exterior space (linked to the right end surface of the plate using RIGID BODY function). Table 6 shows a comparison of ultimate behaviors between two different loading positions. FE model length is 150 mm and solid element type C3D8R is applied to FE model. It is concluded that the ultimate behavior of bolted connections was not affected by the difference of loading position. Considering the run time of analysis shown in Table 6, the former (loading is assigned to the

Table 6
Influence of loading position

Specimen	Loading location	Analysis time (s)	Failure mode	Max. disp δ_{ua} (mm)	Ultimate strength P_{ua} (kN)
SA2-2	Bolt	596	E	14.75	44.42
	Plate end	1181	E	14.75	44.40
SB2-4	Bolt	1511	N	43.05	87.02
	Plate end	6294	N	42.55	86.84
SC2-1	Bolt	1639	E→B	16.10	130.77
	Plate end	3306	E→B	16.05	130.73

Table 7
Influence of model length

Specimen	FE analysis				Experiment		P_{ua}/P_{ue}
	Mesh size T × W (mm)	Model length L (mm)	Failure mode	Ultimate strength P_{ua} (kN)	Failure mode	Ultimate strength P_{ue} (kN)	
SA2-2	$t/2 \times t/2$	90	E	44.38	E	48.05	0.92
		205	**E**	**44.42**			**0.92**
	$t/3 \times t/3$	120	N	86.07			1.01
		150	N	86.81			1.01
SB2-4		180	N	86.84	N	85.62	1.01
		230	**N**	**87.02**			**1.02**
		300	N	86.84			1.01
	$t/3 \times t/3$	72	E→B	131.85			1.14
		102	E→B	131.09			1.13
SC2-1		132	E→B	131.25	E→B	115.62	1.14
		150	E→B	130.92			**1.13**
		230	**E→B**	**130.77**			1.13
SC2-3	$t/3 \times t/3$	150	B	176.97	B	162.34	1.09
		230	**B**	**172.10**			**1.06**
SC2-4	$t/3 \times t/3$	150	B	152.79	B	163.30	0.94
		240	**B**	**153.99**			**0.94**

reference point on the bolt shank) is adopted in this FE analysis.

4.3. Influence of plate model length

Table 7 summaries the results of FE analyses to examine the influence of plate model length on the ultimate behaviors of bolted connections. Solid element type C3D8R is used in FE analysis and failure criterion, FC1 is applied. Model length in Table 7 means connection length from the left free end of plate to the supported end of plate (Fig. 5) and is varied according to specimens. The bold letters in Table 7 specify the FE results of specimens with the effective length, which subtracts grip part length from the whole length of test specimens as mentioned in Section 3.3. Although model length becomes longer, the failure mode obtained from different model length of each specimen is identical to that of test results and the ultimate strength obtained from each FE model shows a slight difference with that of test results, but the variance can be ignored. Consequently, influence of plate model length on the failure mode and the ultimate strength of bolted connections with thin-walled SUS304 steel plates can be

negligible. Thus, this paper recommends 150 mm as a reasonable model length with consideration of bolt arrangement, bolt pitch (p) and end distance (e).

4.4. Estimation of failure mode by FC

Based on the three failure criteria (FC1, FC2 and FC3) presented in Section 3.6, failure modes of each specimen are predicted and the comparison with the test results is summarized in Table 8. Failure modes of FE model estimated by means of FC1 are same as those of the test results. However, for FC2 and FC3, even if the failure modes of specimens SA2-2 and SB2-4 show a good agreement with test results, the FE results of specimens SC2-1, SC2-3 and SC2-4, where two bolts are arranged perpendicular to the direction of load are different from the test results. The reason can be thought that for Series SC with edge distance ($b = 55$ mm), the deformation of width direction is restrained by wide width plate (long edge distance and two rows of bolt arrangements) and high stress concentration in the location ② (see Fig. 6): near bolt hole in contact with bolt shank is revealed. Figs. 7(a)–(c) present the stress/strain-enforced displacement curves for

Table 8
Failure mode estimated by three failure criteria

Specimen	Mesh size T × W (mm)	FE analysis			Experiment
		Failure mode			Failure mode
		FC1	FC2	FC3	
SA2-2	$t/2 \times t/2$	**E**	E	E	E
SB2-4	$t/2 \times t/2$	**N**	N	N	N
SC2-1	$t/2 \times t/2$	**E→B**	E	E	E→B
SC2-3	$t/3 \times t/3$	**B**	E	E	B
SC2-4	$t/3 \times t/3$	**B**	E	E	B

SC2-4 model and the more detailed comparisons of non-dimensional stress and strain, which are normalized by the ultimate stress and strain. In Fig. 7(a), the ratio of direct stress (σ_{11}) versus ultimate stress ($\sigma_{t\ max}$) in location ① comes up to unity (1.0) earlier than that of shear stress (τ_{12}) versus ultimate stress ($\tau_{t\ max}$) in location ②. Tensile fracture occurs at the tension plane of the inmost bolt hole perpendicular to load line and thus, failure mode B is predicted for specimen SC2-4. However, in Figs. 7(b) and (c), equivalent stress (σ_{eq}) and equivalent plastic strain (ε_{eq}^p) of location ② reach ultimate values ($\sigma_{t\ max}$ or $\varepsilon_{t\ max}$), respectively, prior to those of location ① (the center of the drilled bolt hole). Failure mode E that shear fracture precedes is predicted in Series SC specimens. Therefore, it is recommended that in this paper, FC 1 as FC be more valid in predicting accurately the failure mode of bolted connection.

4.5. Comparison of fe analysis results and test results

Up to now, numerical investigation and parametric study to the embody FE model which can predict the failure mode, ultimate strength and curling of thin-walled SUS304 steel bolted connection under shear have been performed with non-linear material, geometrical and contact analysis and thus, the following FE modeling procedures are recommended: (a) element type; solid element (C3D8R, three-dimensional eight-node isoparametric solid element) for FE model of plate and rigid body for bolt model, (b) mesh size; $t/2 \times t/2$ mm (surface by thickness) for model with no curling and $t/3 \times t/3$ mm for model curled, (c) loading method and loading position; enforced displacement control to reference point assigned at bolt shank, (d) FE mode length; 150 mm, (e) failure criteria; FC1 (when direct stress or shear stress obtained from FE analysis in the vicinity of bolt hole reaches the ultimate stress, suppose that the fracture starts). Table 9 represents the comparison of reference test results with FE analysis results based on procedures described above. The FE analysis results for failure mode and ultimate strength were in a good agreement with the test results. Fig. 8 illustrates the typical failure shapes of test results (the upper part) and the stress distribution investigated at the
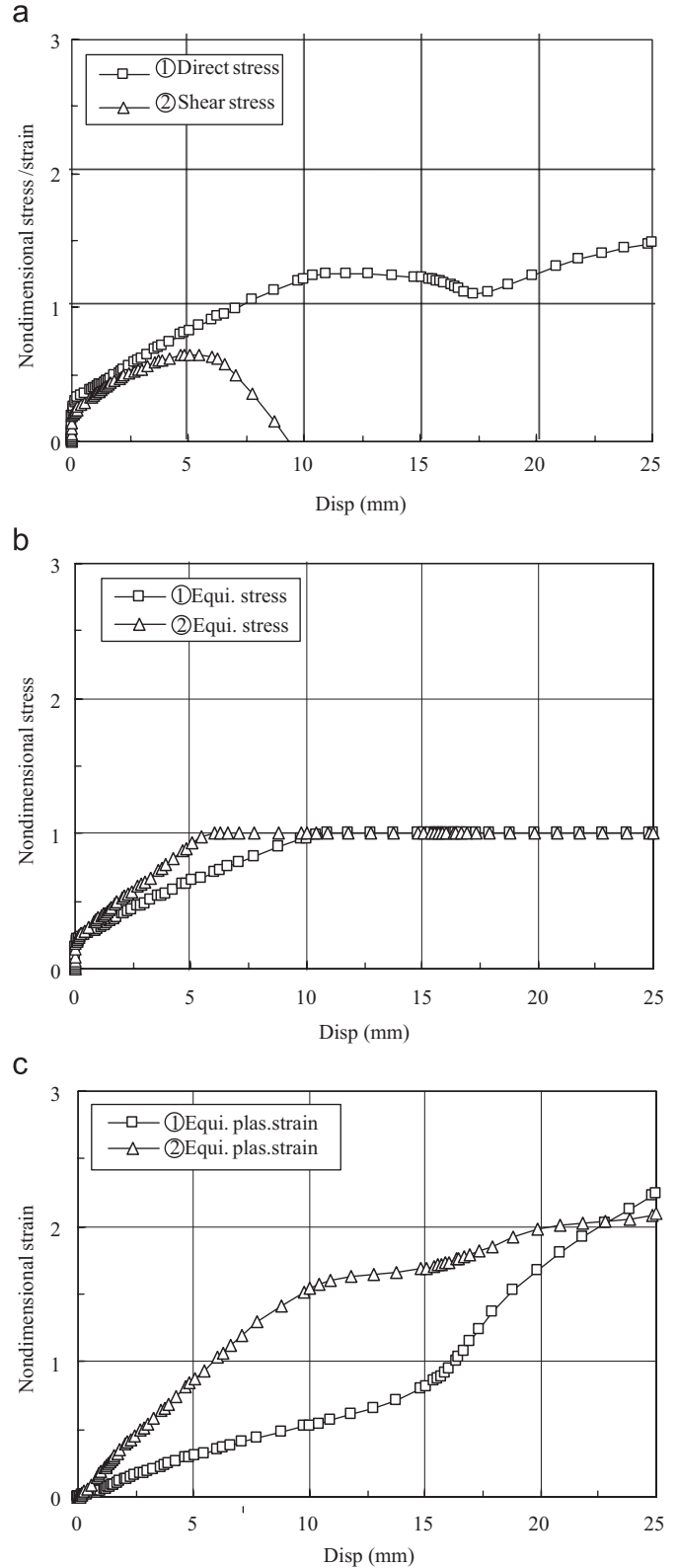
Fig. 7. Comparison of stress or strain at location ①, ②. (a) Direct stress or shear stress at location ①, ②, (b) Equivalent stress at location ①, ②, and (c) Equivalent plastic stress at location ①, ②.

ultimate strength level of each FE model (the lower part) for thin-walled stainless steel bolted connections. From the FE analysis results of Fig. 8, the deformed geometry and

Table 9
FE results compared with test results

Specimen	Nominal thickness (mm)	FE analysis			Experiment		P_{ua}/P_{ue}
		Failure mode	Max. disp. δua (mm)	Ultimate strength P_{ua} (kN)	Failure mode	Ultimate strength P_{ue} (kN)	
SA1-1	1.5	E	8.29	13.58	E	12.28	1.106
SB1-4		N	21.59	43.32	N	43.34	1.000
SC1-4		B	6.08	79.99	B	79.53	1.006
SA2-2	3.0	E	13.21	44.85	E	48.05	0.933
SB2-4		N	25.29	86.81	N	85.62	1.014
SC2-1		E→B	15.63	130.92	E→B	115.62	1.132
SC2-3		B	18.00	176.97	B	162.34	1.090
SC2-4		B	15.56	152.79	B	163.30	0.936
					Mean		1.027
					Standard deviation		0.075
					Coefficient of variation		0.073
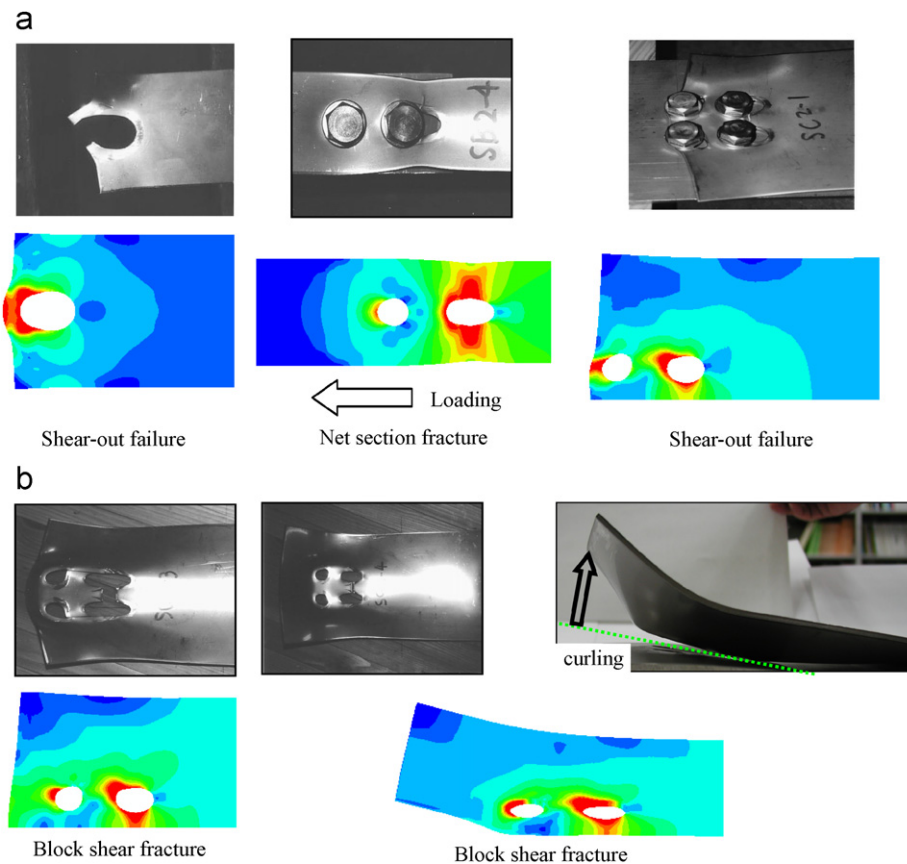
Fig. 8. Typical failure shapes of test specimens (up) and stress distribution of FE analysis at ultimate strength level (down). (a) SA1-1 ($e = 12$, $b = 25$), (b) SB2-4 ($e = 60$, $b = 25$), (c) SC2-1 ($e = 12$, $b = 55$), (d) SC2-3 ($e = 30$, $b = 55$), and (e) SC2-4 ($e = 60$, $b = 55$).

yield zone patterns in bolted connections can be seen. Three types of failure modes in both test results and FE analysis results are observed identically: net section fracture (N), shear-out fracture (E) and block shear rupture (B). Specimens such as SB1-4 and SB2-4, which have relative short edge distance (b), compared with end distance (e) exhibited net section fracture accompanied by necking of the net section farthest from the end of the connection as shown in Fig. 8(b). Secondly, shear-out fracture occurred for specimens SA1-1 and SC2-1 of which end distance (e) is relatively short and it can be seen that the elements from the edge of bolt hole to the end of the plate were protruded by large shear stresses as shown in Figs. 8(a) and (c). Lastly, the failure mode of block shear

Table 10
Influence of curling on the ultimate strength

Specimen	FE analysis			Experiment		P_{ua}/P_{ue}	P_{ua}/P_{uaR}
	Failure mode	Max. disp. δ_{ua} (mm)	Ultimate strenth P_{ua} (kN)	Failure mode	Ultimate strength P_{ue} (kN)		
SB1-4	N	44.43	41.69	N	43.34	0.96	0.96
SB1-4R	N	21.43	43.48	N	43.34	1.00	1.00
SC1-4	B	5.80	79.99	B	79.53	1.01	0.80
SC1-4R	B	13.71	100.23	B	79.53	1.26	1.00
SC2-3	B	18.00	176.97	B	162.34	1.09	1.00
SC2-3R	B	18.15	176.98	B	162.34	1.09	1.00
SC2-4	B	18.81	152.79	B	163.30	0.94	0.75
SC2-4R	B	17.20	202.70	B	163.30	1.24	1.00

rupture is predicted in specimens SC2-3 and SC2-4, where an apparent yield zone of the net section (rupture of net tension plane with necking) between the two bolt holes the farthest from the left end of FE model and a subsequent partial yield zone of the gross shear area (yield/rupture of the shear plane) are observed. From the comparison depicted above, it should be noted that the FE model established in this paper is effective in predicting the ultimate behavior (failure mode and ultimate strength) for bolted connections with thin-walled stainless steel.

4.6. Influence of curling

In order to investigate the influence of curling on the ultimate behavior of bolted connections fabricated from the thin-walled stainless steel plate under shear using FE analysis, the specimens such as SB1-4, SC1-4, SC2-3 and SC2-4 which were curled out of plane in test results as mentioned in Section 3.6.2 are modeled. Two types of FE models per a test specimen are analyzed according to the constraint of curling of plate ends; e.g., FE models such as SB1-4, SC1-4, SC2-3 and SC2-4 in Table 10 mean that curling is not restrained (the edges of plate except support end are free), FE models such as SB1-4R, SC1-4R, SC2-3R and SC2-4R in Table 10 mean that curling is restrained (displacement of thickness direction at the edges of plate is zero). Table 10 summarizes the FE analysis results for eight models and comparison of failure mode and ultimate strength between FE model with free edges and FE model with restrained curling. Fig. 10 represents load–displacement curves of specimens SC2-3, SC2-3R, SC2-4 and SC2-4R, which are divided into two load cases so as to examine the change of strength by influence of curling: one is for the strength sum in the first column of bolt (P1) and the other is for the strength sum in the second column of bolt (P2) as provided in Fig. 9. Failure modes for two types of FE models are the same irrespective of constraint of curling. The ultimate strength ratios (P_{ua}/P_{uaR}) of specimens with curling against specimens with no curling range from 0.75 to 1.00. Other specimen except SC2-3 showed the reduction of ultimate strength by 4–25% compared with specimens with curling restrained: i.e., it is found that

P_1 : strength in the first column of bolt

P_2 : strength in the second column of bolt
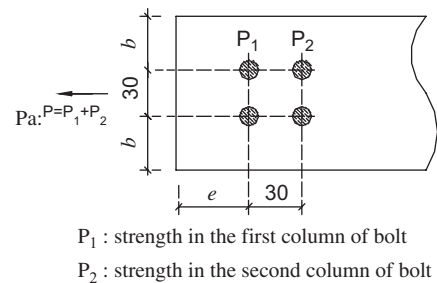
Fig. 9. Definition of the calculation of ultimate strength.

curling has an effect on the ultimate strength of bolted connections and should be considered in estimating the ultimate strength. In addition, it can be seen that for specimen SC2-4, curling is observed before the ultimate strength is reached as shown in Fig. 10(b), while for specimen SC2-3, load–displacement curves is almost identical to that of SC2-3R and the curling seems to occur after the ultimate strength is reached since there is no sharp drop of strength as plotted in Fig. 10(a). Accordingly, the curling of SC2-3 has no effect on the ultimate strength of connection and can be negligible. Fig. 11 presents the deformed shapes and the equivalent stress contours at maximum load for SC2-4 and SC2-4R, respectively.

5. Summary and conclusions

Supplementing the experimental results, the purpose of this research is to predict the ultimate behaviors such as failure mode, ultimate strength and the occurrence of curling for thin-walled stainless steel bolted connections through the FE analysis. Test results of eight specimens with two kinds of plate thickness and three types of bolt arrangements were used to calibrate the FE models. This paper established the FE model which can capture non-linearities including material, geometry and boundary condition (contact) and presented the appropriate procedures of FE analysis mentioned in Section 4.5: i.e., element type, mesh size, loading position, model length and failure criteria. In particular, it was shown that FE analysis results were in a good agreement with test results in terms of
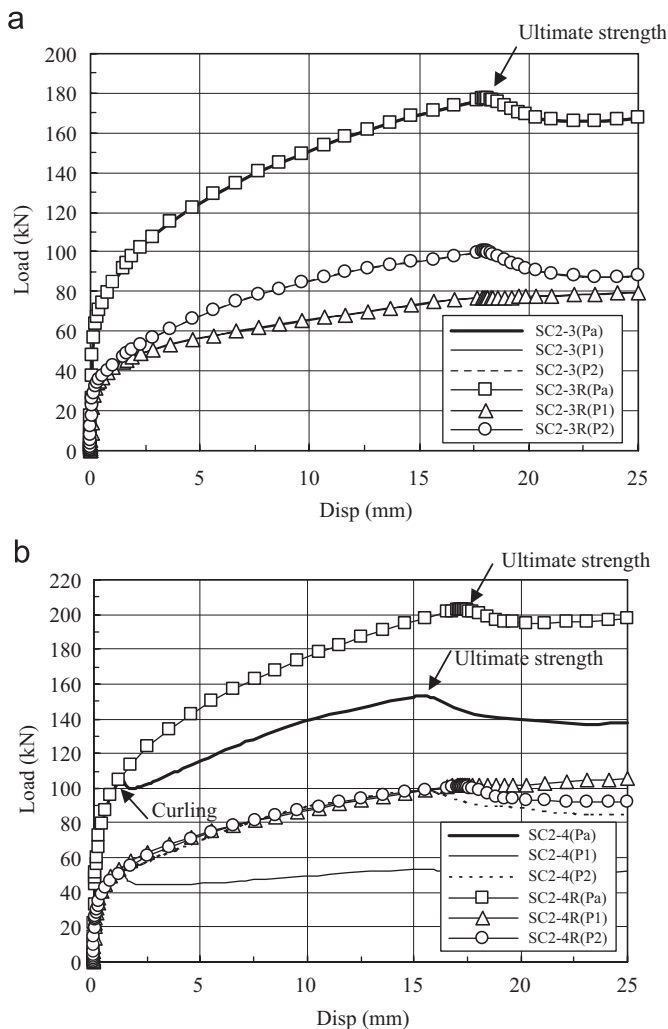
Fig. 10. Influence of curling on the ultimate behavior. (a) Load-Displacement curves of SC2-3 and SC2-3R, (b) Load-Displacement curves of SC2-4 and SC2-4R.
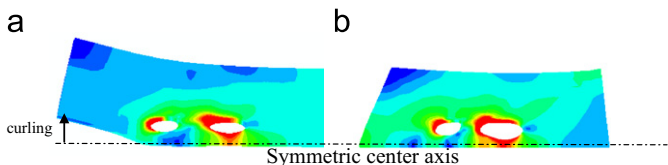
Fig. 11. Deformed shapes and stress contours at ultimate strength. (a) SC2-4, (b) SC2-4R.

failure mode and ultimate strength. The FE model predicted accurately the curling of bolted connections, which was occurred in the experimental results and could also trace the entire load–displacement path. In addition, with the FE analysis results, the yield patterns, deformed shapes and stress/strain distributions in bolted connections were possible to be scrutinized in detail at specified displacement level. A variety of parametric studies were performed in order to investigate the influence of the curling (out of plane deformation) on the ultimate strength

of bolted connections, which has rarely been studied in the previous research. Two types of FE model with curling and no curling according to the restraint of curling of plate in the parametric study were analyzed. FE analysis models in which curling was occurred showed the reduction of ultimate strength by 4–25% when compared with FE models restrained from curling. It should also be noted that if curling is occurred in the FE model after the ultimate strength is reached, the curling has negligible influence on the ultimate strength of bolted connections. In the previous experimental research by Kuwamura et al., they report that modified formula for thin-walled stainless steel (SUS304) are unconservative in estimating the ultimate strength of bolted connections with end curling. Undoubtedly, the current design standards do not also consider sufficiently the influence of curling on the ultimate behavior of bolted connections. Therefore, owing to the validification of FE analysis, it is possible to extrapolate beyond the range of variables used in experimental research and additional research is necessary to further quantify the reduction effect of strength by curling utilizing FE methodology presented in this paper.

Acknowledgments

References

[1] Johnson AL, Winter G. Behavior of stainless steel columns and beams. Journal Structural Division, ASCE Proceedings 1966;92(10): 97–118.

[2] American Iron and Steel Institute. Specification for the design of light gage cold-formed stainless steel structural members, AISI, 1968

[3] American Iron and Steel Institute. Stainless steel cold-formed structural design manual, AISI, 1974

[4] ANSI/ASCE. Cold-formed stainless steel structures. Specification for design of cold-formed stainless steel structural members. ANSI/ASCE-8-90,1990.

[5] European Committee for Standardisation. Design of steel structures: supplementary rules for stainless steels, eurocode 3 Part 1.4,1996.

[6] Australian Standard/New Zealand Standard. Cold-formed stainless steel structures. AS/NZS:4673, 2001.

[7] American Society of Civil Engineers. Specification for the design of cold-formed stainless steel structural members. SEI/ASCE-8-02, 2002

[8] Design and construction standards for stainless steel buildings. Stainless Steel Building Association of Japan (SSBA), 1995 (in Japanese).

[9] The Design and Specifications for stainless steel structures. stainless Steel Building Association of Japan (SSBA), 2001 (in Japanese).

[10] Akoi H. Establishment of design standards and current practice for stainless steel structural design in Japan. Journal of Constructional Steel Research 2000;54:191–210.

[11] Steel Structure Laboratory Experimental Report on Strength of Bolted Connections in Thin-walled Plates. Tokyo: Steel Structure Laboratory, The University of Tokyo; 2001 (in Japanese).

[12] Kuwamura H, Isozaki A. Ultimate behavior of fastener connections of thin stainless steel plates. Journal of Structural and Construction Engineering (Transactions of Architectural Institute of Japan) 2002;556:159–66 (in Japanese).

[13] Kuwamura H, Inaba Y, Isozaki A. Flexural buckling of centrally loaded columns of thin-walled stainless steel—study on light-weight stainless steel structures Part 2. Journal of Structural and Construction Engineering Transactions of Architectural Institute of Japan 2001;549:135–42 (in Japanese).

[14] Kuwamura H, Inaba Y, Isozaki A. Local buckling and effective width of thin-walled stainless steel members. The third international conference on thin-walled structures 2001:209–16.

[15] Kuwamura H, Inaba Y, Isozaki A. Local buckling and effective width of thin-walled stainless steel stub-columns-study on light-weight stainless steel structures Part 1. Journal of Structural and Construction Engineering Transactions of Architectural Institute of Japan 2001;544:155–62 (in Japanese).

[16] Design manual of light-weight stainless steel structures. Stainless Steel Building Association of Japan (SSBA), 2006 (in Japanese).

[17] Chung KF, Ip KH. Finite element modeling of bolted connections between cold-formed steel strips and hot rolled steel plates under static shear. Engineering Structures 2001;22:1271–84.

[18] Fan L, Rondal J, Cescotto S. Finite element modeling of single lap screw connections in steel sheeting under static shear. Thin-Walled Structures 1997;27(2):165–85.

[19] ABAQUS, Inc. ABAQUS. Ver.6.4. analysis user's manual, 2003.

[20] Hibbitt, Karlsson & Sorensen, Inc. ABAQUS Theory Manual Ver.5.8., 1998.

[21] Barth KE, Orbison JG, Nukala R. Behavior of steel tension members subjected to uniaxial loading. Journal of Constructional Steel Research 2002;58:1103–20.

[22] Lim JBP, Nethercot DA. Stiffness prediction for bolted moment-connections between cold-formed steel members. Journal of Constructional Steel Research 2004;60(1):85–107.

[23] Bursi OS, Jaspart JP. Basic issues in the finite element simulation of extended end plate. Computers & Structures 1998;69:361–82.

[24] Kamei Y, Ikehata B, Nishimura N. An analytical study on classification of limit states of hsfg bolted joints in tension. Journal of Structural and Earthquake Engineering Japan Society of Civil Engineers (JSCE) 1998;584/I-42:243–53 (in Japanese).

[25] Emi T, Tabuchi M, Tanaka T, Namba H, Nagatani Y. Elasto-plastic behavior of high strength friction joints. Steel Construction Engineering of Japanese Society of Steel Construction (JSSC) 2003;10(39):11–22 (in Japanese).

[26] Aceti R, Ballio G, Capsoni A, Corradi L. A limit analysis study to interpret the ultimate behavior of bolted joints. Journal of Constructional Steel Research 2004;60(9):1615–35.

[27] Moriyama T, Kuzuu T, Uematsu Y, Yamada M. FEM analysis of three-dimensioned elastoplastic and contact problem on high strength bolt friction joint. Proceeding of Annual Meeting Architectural Institute of Japan (AIJ), 1997; 253-254 (in Japanese).

[28] Epstein HI, McGinnis MJ. Finite element modeling of block shear in structural tees. Computers & Structures 2000;77(5): 423–599.

[29] Kim HJ, Yura JA. The effect of ultimate-to-yield ratio on the bearing strength of bolted connections. Journal of Constructional Steel Research 1999;49:255–69.

[30] Chung KF, Ip KH. Finite element investigation on the structural behavior of cold-formed steel bolted connections. Engineering Structures 2001;23:1115–25.

[31] Orbison JG, Wagner ME, Fritz WP. Tension plane behavior in single-row bolted connections subject to block shear. Journal of Constructional Steel Research 1999;49(3):225–39.

[32] Topkaya C. A finite element parametric study on block shear failure of steel tension members. Journal of Constructional Steel Research 2004;60(11):1615–35.

[33] Winter G. Tests on bolted connections in light gage. Journal Structural Division, ASCE, 1956; 82(2):920-1–920-25.

[34] Chong KP, Matlock RB. Light-gage steel bolted connections without washers. Journal Structural Division, ASCE 1975;101(7): 1381–91.